Metabarcoding Reveals High Diversity of Benthic Foraminifera Driven by Atlantification of Coastal Svalbard

Ngoc-Loi Nguyen (loinguyen@iopan.pl)
Institute of Oceanology Polish Academy of Sciences
Joanna Pawłowska
Institute of Oceanology Polish Academy of Sciences
Inès Barrenechea Angeles
Department of Earth Sciences, University of Geneva
Marek Zajaczkowski
Institute of Oceanology Polish Academy of Sciences
Jan Pawłowski
Department of Earth Sciences, University of Geneva

Research Article

Keywords: Benthic foraminifera, sedimentary DNA, metabarcoding, Svalbard, atlantification

Posted Date: December 2nd, 2021

DOI: https://doi.org/10.21203/rs.3.rs-1009107/v1

Metabarcoding reveals high diversity of benthic foraminifera driven by atlantification of coastal Svalbard

Ngoc-Loi Nguyen[1*], Joanna Pawłowska[1], Inès Barrenechea Angeles[2,3], Marek Zajaczkowski[1], Jan Pawłowski[1,3]

[1] Institute of Oceanology Polish Academy of Sciences, Powstancow Warszawy 55 81-712 Sopot, Poland

[2] Department of Earth Sciences, University of Geneva, Rue des Maraîchers 13, 1205 Geneva, Switzerland

[3] Department of Genetics and Evolution, University of Geneva, Boulevard d'Yvoy 4, 1205 Geneva, Switzerland

* Correspondence to: loinguyen@iopan.pl, Tel.: +48 (58) 7311 661

Abstract (300 words)

Arctic marine biodiversity is undergoing rapid changes due to global warming and modifications of oceanic water masses circulation. These changes have been demonstrated in the case of mega- and macrofauna, but much less is known about their impact on the biodiversity of smaller size organisms, such as foraminifera that represents a main component of meiofauna in the Arctic. Several studies analysed the distribution and diversity of Arctic foraminifera. However, all these studies are based exclusively on the morphological identification of specimens sorted from sediment samples. Here, we present the first assessment of Arctic foraminifera diversity based on metabarcoding of sediment DNA samples collected in fjords and open sea areas in Svalbard Archipelago. We obtained a total of 5,968,786 reads that represented 1,384 ASVs. More than half of the ASVs (51.7%) could not be assigned to any group in the reference database suggesting a high genetic novelty of Svalbard foraminifera.

The sieved and unsieved samples resolved comparable communities, sharing 1023 ASVs, comprising over 97% of reads. Our analyses show that the foraminiferal assemblage differs between the localities, with communities distinctly separated between fjord and open sea stations. Each locality was characterized by a specific assemblage, with only a small overlap in the case of open sea areas. Our study demonstrates a clear pattern of the influence of water masses on the structure of foraminiferal communities. The stations situated on the western coast of Svalbard that is strongly influenced by warm and salty Atlantic Water (AW) are characterized by much higher diversity than stations in the northern and eastern part, where the impact of AW is less pronounced. This high diversity and specificity of Svalbard foraminifera associated with water mass distribution indicate that the foraminiferal metabarcoding data can be a very useful tool for inferring present and past environmental conditions in the Arctic.

Keywords (4 to 6 keywords)

Benthic foraminifera, sedimentary DNA, metabarcoding, Svalbard, atlantification

1. Introduction

The Arctic Ocean is strongly impacted by the increased influence of warm and saline Atlantic Water, so-called "atlantification", which causes sea-ice retreat and sea surface temperature increases [1-3], directly affecting the entire ecosystem. Such changes in physical drivers lead to shifts of Atlantic species ranges towards the Arctic [4], increase in productivity [5], and changes in the timing of spring phytoplankton bloom [6]. These changes may create shifts in food webs, affecting planktonic and bottom communities [6,7]. Particularly, Svalbard ecosystems are currently affected by increased heat transport from northward-flowing currents [3,8-10]. The changing environmental conditions in this region introduces a significant impact on shaping biodiversity and the biogeography of many taxonomic groups, such as birds and mammals [11,12], fish [13,14], zooplankton [15-17], phytoplankton [18,19], and planktonic foraminifera [20,21].

Foraminifera are a major component of benthic communities, from transitional and marine coastal areas to the deep-sea zones, where they have been demonstrated to be of significant importance in terms of both high abundance and diversity [22-24]. Benthic foraminifera are recognized as important ecological indicators of environmental stress because they are particularly sensitive to abrupt climate change [25-27].

Traditionally, the morphological observations of foraminiferal mineral shells (so called tests), which belong to either the class Tubothalamea or Globothalamea, are the basic feature used to assess foraminiferal diversity. However, morphological identification is time-consuming and expertise-demanding, making it costly and unpractical, particularly for large-scale surveys. Recently, the metabarcoding of environmental DNA (eDNA) samples have provided new insights into biodiversity and ecological distribution of numerous taxonomic groups and offer an alternative to the traditional morphology-based approach [28-30]. Metabarcoding consists in high-throughput sequencing of short DNA barcodes that include enough information for species identification to get a comprehensive inventory of all organisms

63 present in a given sample, e.g., foraminiferal sequences derived from the 37f hypervariable
64 region of the 18S small subunit (SSU) rRNA gene [31,32]. To better understand large-scale
65 patterns of biodiversity and distribution in various groups, this method is increasingly being
66 employed, particularly in marine environments [22,29,33,34]. While numerous foraminiferal
67 metabarcoding studies were conducted in various coastal areas [35-38], and the deep-sea [22,39-41];
68 the application of eDNA metabarcoding to monitor foraminiferal diversity in the Arctic was
69 limited to a few paleogenomic studies using foraminifera as proxies in palaeoceanographic
70 reconstructions [42-44].

71 In the conventional morphology-based foraminiferal studies the sediment samples are
72 sieved before the specimens are sorted. In metabarcoding approaches, the DNA is also
73 extracted from sieved sediment samples, which has several benefits: potentially reducing
74 sample heterogeneity, detecting completely small and low abundant taxa, achieving a higher
75 number of reads, or decreasing primer bias due to the reduction in the amount of DNA template
76 produced by the large specimens [45,46]. Some DNA metabarcoding studies have shown that the
77 preprocessing of samples does not significantly alter metazoan diversity patterns [47,48].
78 However, the effectiveness of sieving versus non-sieving in the case of foraminiferal
79 metabarcoding has not been examined yet.

80 The two main goals of this study are to investigate whether metabarcoding of sieved
81 sediment is effective for the assessment of foraminiferal biodiversity and how the foraminiferal
82 communities respond to rapid environmental shifts of Arctic marine ecosystems. Taxonomic
83 composition, diversity, and distribution of benthic foraminifera were analyzed in fjords and
84 open water areas in Svalbard in order to 1) compare species composition and diversity patterns
85 inferred from sieved and unsieved sediment samples, 2) describe the spatial diversity of
86 Svalbard foraminiferal communities, and 3) identify new potential bioindicators of
87 atlantification.

2. Study area

The oceanography of Svalbard region is shaped mainly by the interplay between warm and saline Atlantic Water (AW) and cold Arctic Water (ArW), as well as locally formed water masses [16,49]. AW is transported northward along the Spitsbergen shelf edge as the West Spitsbergen Current (WSC, Fig. 1) [50,51]. WSC is one of the major heat contributors to the Arctic Ocean[52], transporting heat from low latitudes into the Arctic and transferring it to the atmosphere and adjacent water masses [53]. Between 78°N and 80°N, the WSC bifurcates into an eastern (Svalbard) branch and a western (Yermak) branch [54]. The Svalbard Branch flows northeasterly, staying close to the continental margin of Svalbard [54]. The Yermak Branch streams northwards and further recirculates southward as the Return Atlantic Current [55]. The Svalbard area is also under the influence of cold Arctic Water (ArW) that is transported from the north-eastern Barents Sea by the East Spitsbergen Current (ESC), also called Sørkapp Current or the Coastal Current [56]. Mixing of ArW and AW results in the formation of Transformed Atlantic Water (TAW) which expanded across the shelf and penetrated the fjords [49,57].

Isfjorden (IS) and Wijdefjorden (WIJ) are located on the west coast Spitsbergen, along the main pathway of AW inflow. Both fjords are linked directly to shelf and slope area [10,58] and therefore, their oceanographic conditions are shaped mainly by the inflow of AW and TAW. Isfjorden is considered to be the most AW-impacted fjord of Spitsbergen [57]. Rijpfjorden (RIJ) is a north-facing fjord, located on the northern coast of Nordaustlandet. The oceanography of Rijpfjorden is dominated by cold ArW, with a less pronounced impact of AW. However, episodic inflows of AW may occur in ice-free periods. As such, it is considered to be a typical Arctic fjord. In most of the year, Rijpfjorden is covered by sea ice and/or drifting ice packs [59].

The southeastern Nordaustlandet (NAL) and the eastern Edgeøya (EDG) are strongly impacted by the presence of large ice caps, making them one of the largest glacierized areas of Svalbard [60]. The tidewater cliffs supply the surrounding areas with large amounts of turbid meltwater [61]. Water masses around Nordaustlandet and Edgeøya are dominated by ArW, carried by the ESC. However, in periods of strong WSC activity, the presence of AW is also pronounced [62].

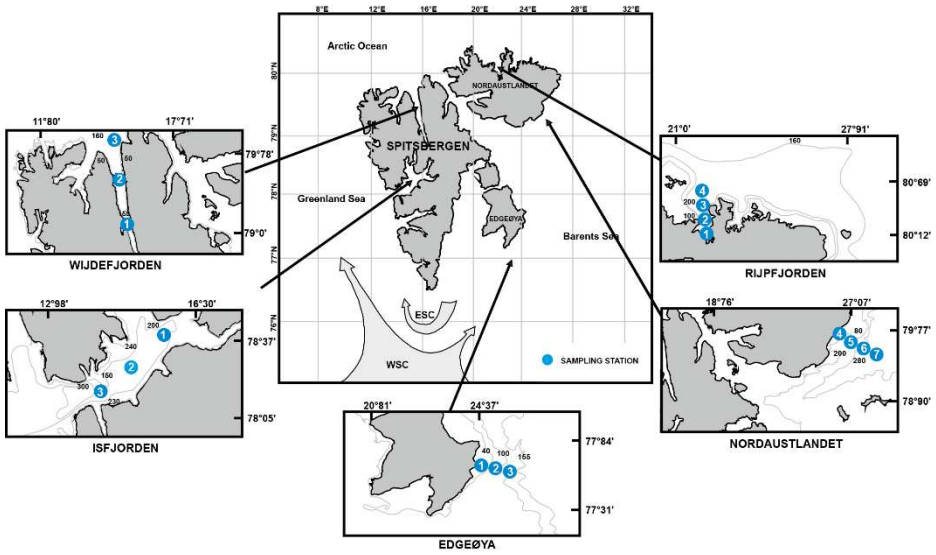

Figure 1. Map showing the location of sampling stations. Abbreviations: WSC - West Spitsbergen Current; ESC - East Spitsbergen Current.

3. Material and Methods

3.1. Sampling

The samples were collected at 15 sampling stations from five localities at Western, Northern and Eastern sides of the Svalbard Archipelago (Fig. 1), including three fjord sites (Isfjorden, Wijdefjorden, Rijpfjorden) and two open marine areas in front of tidewater glaciers (Edgeøya, Nordaustlandet). Sampling stations coordinates and sampling depths can be found in Table S1. Surface sediment samples were collected with the use of a box corer during the

129 cruise of R/V *Oceania* in August 2016. The upper 2 cm of sediment has been sampled from
130 the surface of approximately 50 cm^2. Samples for sedimentary eDNA analysis were split into
131 two: one half remained unsieved and the other half has been wet sieved on 500 μm, 100 μm,
132 and 63 μm sieves. A fraction smaller than 63 μm was retained. Samples were transferred to
133 sterile containers and frozen at −20°C. In each sampling station, physical properties of the
134 water column from a vertical conductivity-temperature-depth (CTD) profiler were obtained
135 using a Mini CTD Sensordata SD202 at intervals of 1 second. Water temperature was reported
136 in degrees Celsius (°C), turbidity was presented in Formazine Turbidity Units (FTU). Water
137 masses were classified according to Cottier, et al. [49]. Supplementary Table S2 contains detailed
138 information.
139
140 **3.2. Metabarcoding analyses**
141 For the sieved samples, the genomic DNA from size fractions >500 μm, 500-100 μm,
142 and 100-63 μm were extracted from 0.25 g of sediment sample with DNeasy PowerSoil Kit
143 (Qiagen, Hilden, Germany). The sediment fraction < 63 μm and the unsieved part were
144 extracted using DNeasy PowerMax Soil Kit (Qiagen, Hilden, Germany), which allows for the
145 process of up to 10 g of sediment. In total, five amplicon libraries per station were prepared,
146 corresponding to the fractions > 500 μm, 500-100 μm, 100-63 μm and < 63 μm, as well as
147 unsieved sample.
148 The foraminifera-specific 37f hypervariable region of 18S rRNA gene was PCR
149 amplified with the primers s14F1/s15 [31,44], tagged with unique sequences of 5 nucleotides
150 appended at 5' ends. Primer sequences and PCR conditions are detailed in Table S3. For each
151 sample, 3 PCR replicates were obtained. PCR products were visualized by 1.5% agarose gel
152 electrophoresis, quantified with Qubit 3.0 fluorometer (Thermo-Fisher Scientific Inc.,
153 Waltham, MA, USA), and the pool was purified with High Pure PCR Cleanup Micro Kit

(Roche Diagnostics GmbH, Mannheim, Germany). Library preparation was performed with TruSeq® DNA PCR-Free LT Library Prep Kit (Illumina Inc., San Diego, CA, USA) and was loaded onto a MiSeq instrument for a paired-end HTS run of 2 × 150 cycles using a v2 kit.

3.3. Data quality control and processing

Bioinformatics analyses were performed using the web application SLIM [63]. The reads were first demultiplexed using the double tag demultiplexing algorithm based on their unique barcode sequences. DADA2 [64] was used for quality trimming and filtering sequences, de-replicating sequences, inferring amplicon sequence variants (ASVs), merging of forward and reverse sequences, and detection and removal of chimeras. A raw number of sequence reads were published by Pawłowska, et al. [65]. Subsequently, all the resulting ASVs tables were curated with the LULU algorithm [66] to remove erroneous ASVs following the online tutorial (https://github.com/tobiasgf/lulu) with default parameters. Final quality filtering of ASVs involved the removal of unique (occurring in only one sample) and rare ASVs (having less than 10 reads).

The remaining ASVs were compared to the curated database of foraminiferal 18S rDNA sequences [67,68] and the PR2 database v4.11.1 [69] using VSEARCH, implemented in SLIM, and BLASTN [70] based on minimum similarity (-perc_identity 80%) and minimum coverage (–qcov_hsp 80%) for the taxonomic assignment to six taxonomic levels (phylum; class; order; family; genus; species). The representative sequences of ASVs that remained unclassified with the foraminiferal database, were aligned in a stand-alone BLAST using BLAST (v2.7.1) search against the NCBI's non-redundant nucleotide database. The sequences diverging by less than 1% were considered as belonging to the same species/genus. ASVs below 99% identity were classified at the family, order, or class or as unassigned foraminifera.

178 Finally, taxonomic compositions in terms of cluster abundance were compared among
179 processing methods only using clusters reliably assigned at the species/genus level.
180
181 **3.4. Statistical analysis**
182 Before statistical analyses, the sample matrix was filtered to remove ASVs that were
183 classified as planktic, or non-foraminifera. For each sample, datasets of 4 size fractions were
184 combined as a sieved dataset and compared to an unsieved dataset in further analysis. All
185 statistical analyses were performed in R, version 4.1.0 [71]. All formal hypothesis tests were
186 conducted on the 5% significance level ($\alpha = 0.05$).
187 To compare the community composition among methods and size fractions, Venn
188 diagrams were constructed using *venn* package [72]. The ASVs rarefaction curves were
189 calculated to visualize whether or when a plateau was reached based on the number of
190 eventually retained ASVs and reads using the iNEXT package [73]. We analyzed differences in
191 the beta-diversity of the community composition by calculating a Non-Metric Multi-
192 Dimensional Scaling (nMDS) on Bray-Curtis similarity coefficient using *vegan* package [74] and
193 a heatmap based on the Spearman's correlation with *pheatmap* package [75]. The influences of
194 environmental factors were calculated with the *envfit* function. A global one-way analysis of
195 similarities (ANOSIM) and permutational multivariate analysis of variance (PERMANOVA)
196 were computed using the function *anosim*, *adonis* and *envfit* with 999 permutations and the
197 Bray-Curtis distance matrix to test whether there were significant differences in community
198 composition among methods and locations of sampling units using log10(1+x) transformed
199 read abundance data.
200 Finally, Sparse Partial Least Squares (PLS) regression, available in the *mixOmics*
201 package [76,77], was used for the multivariate analysis of the combined foraminiferal datasets at
202 ASVs level to identify ASVs that were more predictive of the observed environmental

response. Pairwise similarity matrices of an sPLS model with 2 components were computed and displayed by *cim* function. This approach enabled us to identify high correlations between certain ASVs and environmental parameters but without considering the structure of the foraminiferal community.

3.5. Data availability

All raw sequencing reads have been deposited in the NCBI Short Read Archive (SRA) database under Bioproject accession number PRJNA768352.

4. Results

4.1. CTD data

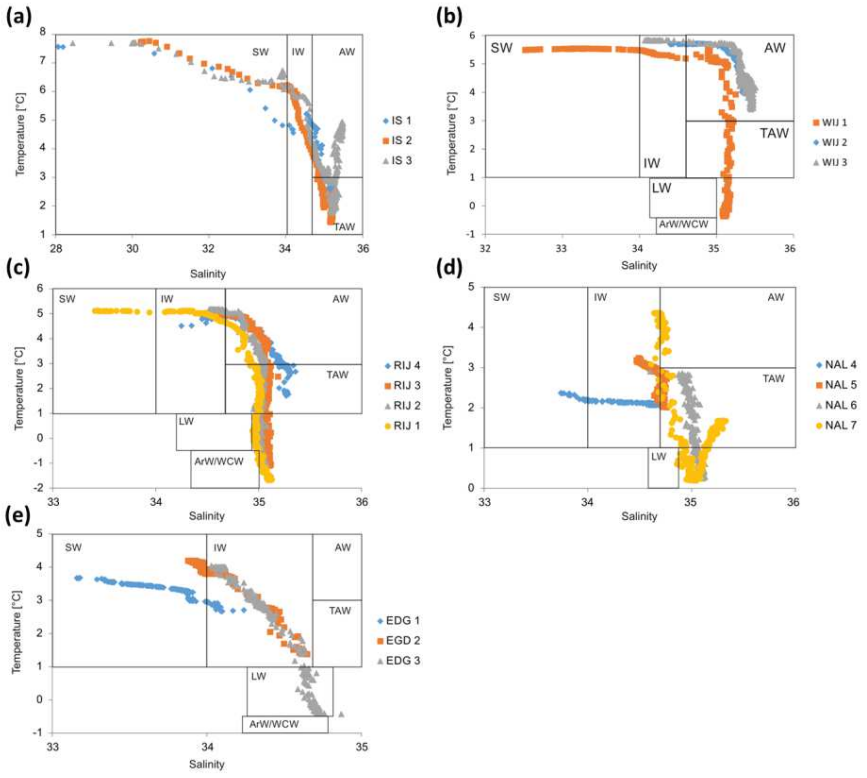

Figure 2. Temperature (°C) and salinity in Svalbard stations: **(a)** IS - Isfjorden, **(b)** WIJ - Wijdefjorden **(c)** RIJ - Rijpfjorden, **(d)** NAL-Nordaustlandet and **(e)** EDG - Edgeøya. Abbreviations: AW- Atlantic Water; TAW- Transformed Atlantic Water; ArW- Arctic Water;

WCW- Winter Cooled Water; SW- Surface Water, LW - Local Water, IW - Intermediate water. Water masses are classified after Cottier et al. [49].

Temperature, salinity, and turbidity for all sampling stations are presented in Figs. 2 and S1, respectively. AW and TAW dominated the water masses in Isfjorden (Fig. 2a) and Wijdefjorden (Fig. 2b), which have the highest temperatures and salinities of the investigated stations. Additionally, Surface Water (SW) and Intermediate Water (IW) were recorded at all stations in Isfjorden and station WIJ1**.** In Isfjorden, the highest temperature of 7.7°C was observed at the surface and progressively decreased towards the bottom to 1.4°C. Similarly, the temperature fluctuated from 5.8°C at the surface to - 0.4°C near the bottom of Wijdefjorden. Water temperatures above 0°C were noted up to 111 m depth at the station WIJ1 and in the whole water column at other stations. Salinity was the lowest at the surface, reaching 28.1 in Isfjorden and 32.5 in Wijdefjorden, respectively. The lowest salinity was recorded at inner Isfjorden and Wijdefjorden (IS1 and WIJ1) and the highest values near the mouth of these fjords (IS3 and WIJ3). The turbidity increased from the inner fjord (0.1 FTU) towards the fjord's mouth (particularly up to 12.5 FTU) in Isfjorden, reaching its maximum in the surface water at the station IS3**.** In contrast, turbidity was the highest in the surface layer and decreased from the inner fjord towards the fjord mouth, ranging from 5.2 to 0.1 FTU.

Rijpfjorden was characterized by the lowest near-bottom temperatures (as low as -1.7 °C) among the studied fjords. Three sites (RIJ1, RIJ2, and RIJ3) reported cold and saline Winter Cooled Water (WCW) in addition to other water masses (AW, TAW, SW, and IW). The temperature ranged from 5.2°C at the top to -1.7°C near the bottom, with the salinity varying from 33.4 to 35.4 throughout the water mass. The lowest near-bottom temperature was noted at the station RIJ1. The water temperature of the whole water column was observed to

be above 0°C at station RIJ4. Turbidity reached over 12.5 FTU at the station RIJ 3 in the near-bottom water layer and decreased to 0.1 FTU towards the mouth of the fjord.

In the region of eastern Svalbard, the Nordaustlandet stations were generally under influence of TAW, whereas AW was noted only at the glacier-distant station NAL7. NAL4 was the sole station where neither TAW nor AW was detected. SW and IW were other water masses recorded near the Nordaustlandet. Water temperature oscillated between 4.4°C at the surface to 0.2 °C near the bottom. Salinity at the surface ranged from 33.6 to 35.3 and increased towards the glacier-distant stations. The water column had relatively low turbidity (<1 FTU). The only exception was glacier-proximal station NAL 4, where turbidity reached 54.8 FTU, which was the highest value of all studied sites.

Edgeøya stations were the most distinct locations, with the absence of Atlantic-origin waters. The IW was detected at all stations, while Local Water (LW) occurred only at station EGD3. Towards the bottom of the stations, the temperature in the water column varied between 4.2 °C and -0.5°C and salinity ranged from 33.2 to 34.9. The highest turbidity was recorded at EGD1, it increased with depth to reach 48.8 FTU near the bottom. At the other stations, turbidity values oscillated from 0.3 to 4.3 FTU.

4.2. Metabarcoding data

We obtained a total of 5,968,786 raw paired-end reads. After bioinformatic processing, the numbers of the raw reads were reduced to 5,579,202 with 4,836,419 in a sieved dataset, and 742,783 in an unsieved dataset. The number of reads per sample is indicated in Table S4. One sample, unsieved IS2, produced a low number of reads and was not included in the analysis of foraminiferal diversity. After LULU curation step and strict filtering of ASVs, 1384 ASVs (1354 ASVs of sieved and 1053 ASVs of unsieved samples) representing 5,483,500 reads

(98.28% of the total reads count) were retained for downstream analysis. The average number of sequences per station were 317,306 for the sieved and 51,976 for the unsieved datasets.

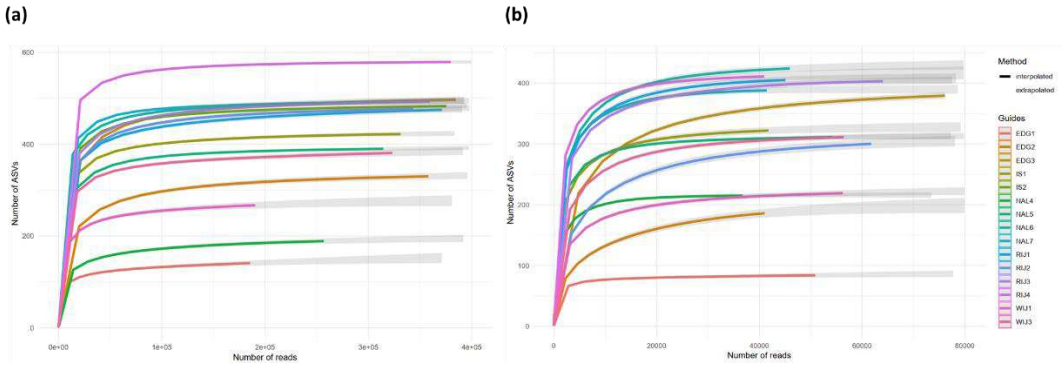

Figure 3. Rarefaction curves showing the relationship between sequencing depth and species richness in amplicon sequence variant (ASVs) of the 37f libraries from 15 stations of **(a)** unsieved (combined fractions) and **(b)** sieved samples.

The rarefaction curves were plotted at the sample level based on the number of retained ASVs and reads (Fig. 3). The rarefaction curves showed that the filtered ASV datasets reach saturation levels, indicating that most of the diversity had been captured and allowing for richness comparison among samples for all individual stations of each location and both methods. Considering the accumulation of ASVs richness across two datasets, sieved datasets exhibited the higher saturation degree of samples, respectively, and the diversity of NAL, IS, RIJ stations are higher than the individual station of EDG and WIJ.

4.3. Taxonomic composition of foraminiferal metabarcodes

Overall, the retained sequences were assigned to 1,384 foraminiferal ASVs. Among them, 758 ASVs were assigned to the class Monothalamea, 252 ASVs were assigned to the class Globothalamea and only 14 ASVs were assigned to the class Tubothalamea (Table S5). The 360 ASVs, classified as Foraminifera_X, had low similarity levels or were mainly assigned

to environmental sequences, that possibly represent non-described taxa. More than half of the ASVs (51.73%) were assigned with low similarity (< 0.9).

Figure 4. Proportions of reads **(a)** and ASVs **(b)** assigned to different foraminiferal classes detected in sieved and unsieved samples at different sites.

The sieved and unsieved sediment DNA samples resolved comparable communities at the class level (Fig. 4). Pairwise comparisons indicated no overall significant differences in community composition between sieved and unsieved datasets (ANOSIM statistic R <0, p > 0.05 and PERMANOVA, Table S6). In Fig. 5a, the Venn diagram showed that 1023 ASVs (corresponding to 97.23% of the reads) were shared among sieved and unsieved samples. The sieved dataset had 331 unique ASVs, while unsieved dataset comprised only 30 unique ASVs (corresponding to 0.1 and 2.67 % of the reads, respectively).

Taxonomic composition in sieved samples noticeably changed between size fractions (Figs. 5b,c). The < 63 µm fraction comprises 1151 ASVs, corresponding to 83% of ASVs (Fig. 5b). It also recovered more unique ASVs (177, corresponding to 13.07 % of ASVs) than any other fractions. Shared foraminiferal ASVs among fractions including 424 ASVs (corresponding to 82.39% of the reads), mostly belonged to Monothalamea (59.72%), and Globothalamea (Rotaliida 25.17%, Textulariida 10.60%) as shown in Fig. S2. In all fractions (Fig. 5c), the monothalamous taxa made up from 58% to 80% of reads. Non-described monothalamiids dominated in the 500-100 µm and < 63 µm fractions (30.48 % and 33.85% of reads, respectively). For multichambered globothalamids, order Textulariida accounted for 15% to 20% of the reads in 500-63 µm fractions, while Rotaliida represented more than 20% of reads in > 63 µm fractions. Interestingly, most reads of unique ASVs were assigned to specific foraminiferal groups in each fraction, e.g., Foraminifera_XX (70.69%) in > 500 µm fraction, Rotaliida (66.21%) in 500 - 100 µm fraction, Textulariida (39.28%) in < 63 um fraction, and Clade Y of Monothalamea (70.24%) in 100 - 63 um fraction, see Fig. S2.

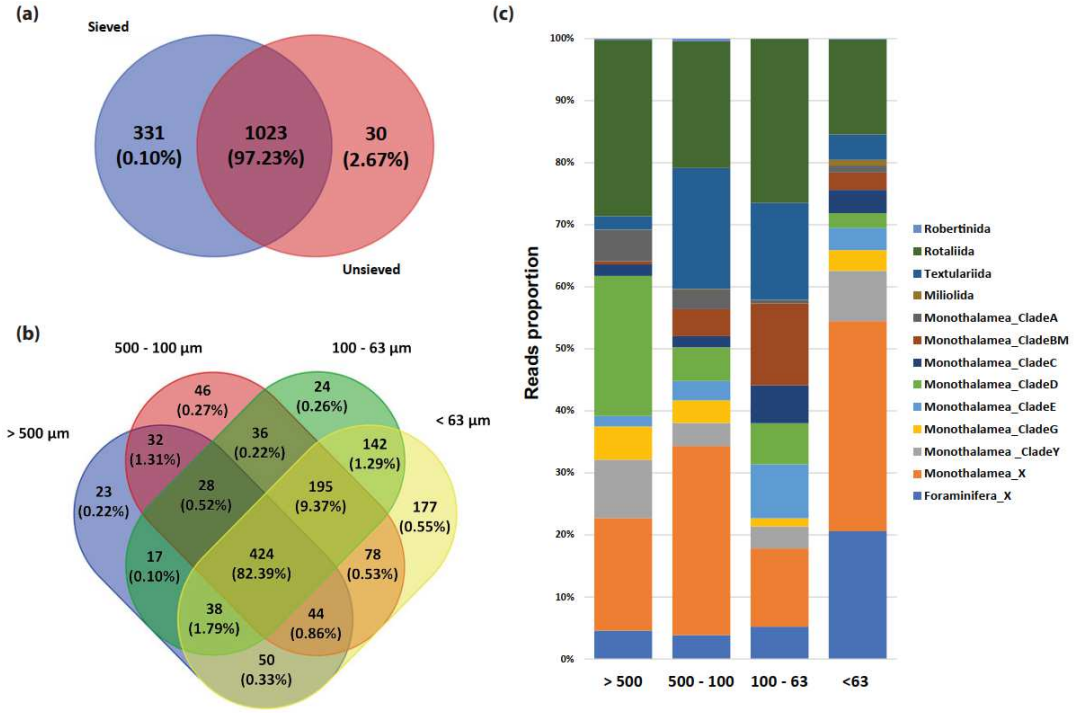

Figure 5. Venn diagrams showing the shared and unique numbers ASVs and proportion of reads for the sieved (combined fractions) and unsieved samples **(a)**, and between different size fractions **(b).** Bar plots represent the proportion of reads assigned to the taxonomic composition of each fraction by order/clade **(c).**

The taxonomic composition of benthic foraminifera also changed between the locations. At the class level (Fig. 4), the monothalamous taxa were the dominant group which accounted for an average of 56.06 % and 61.77% of total ASVs and reads in both datasets, respectively. The highest proportion of monothalamiids (95.80%) was observed at the station EDG1 in the sieved dataset. The contribution of monothalamiids decreased in the deeper EDG stations in favour of the class Globothalamea. Comparatively, the average proportions of ASVs and reads assigned to Globothalamea were 22.60% of the ASVs and 30.75% of reads, respectively. The highest relative abundance of Globothalamea (80.80%) occurred in the WIJ3_Sieved sample. The Tubothalamea represented only a minor part of the total community (0.06% of ASVs and 7.42% of reads on average).

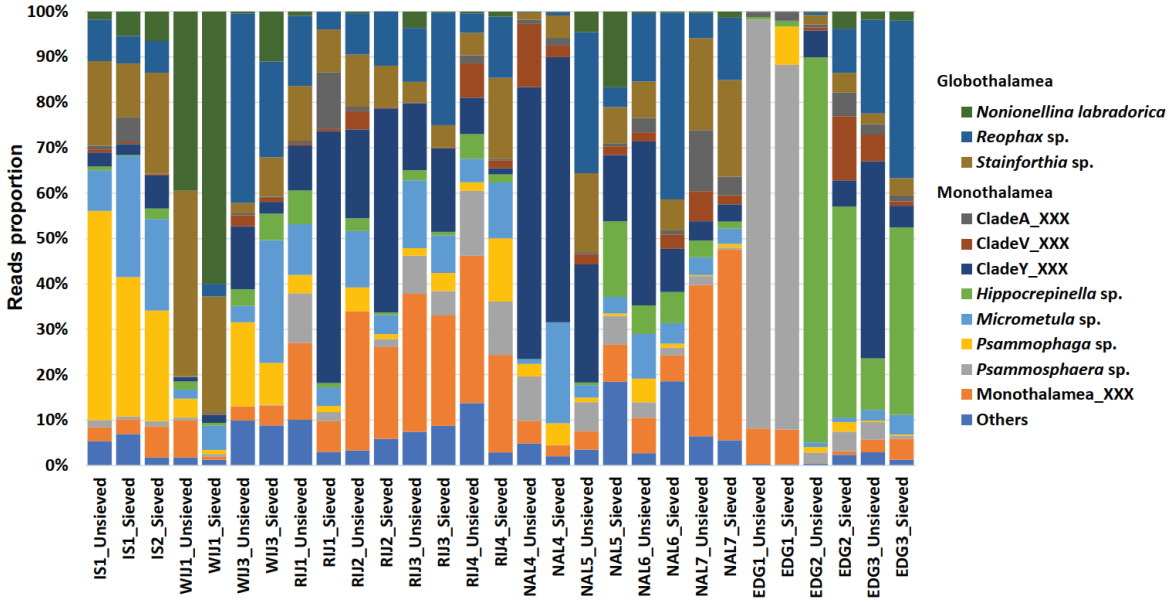

Figure 6. Patterns of relative abundance of dominant genera and species in the sieved (combined fractions) and unsieved sediment samples for each location.

The variations of foraminiferal assemblage between different sampling localities were also reflected in the taxonomic composition of foraminiferal assemblages at the lower taxonomic level. To compare species composition in each station, all ASVs which had an identity percentage with the reference database of more than 99% and no less than 10 reads were picked and those attributed to the same taxa were merged (Fig. 6).

In the stations located at the western coast of Spitsbergen (IS, WIJ), foraminiferal communities were dominated by genera *Psammophaga* and *Micrometula*, which together made up to 57.35% of reads. The WIJ1 was the only station where the majority of sequences belonged to a textularid *Reophax* sp. and a rotalid *Stainforthia* sp. Another rotalid species *Nonionellina labradorica* was present at all IS and WIJ stations, mainly distributed in WIJ1 (sieved: 59.99%, unsieved: 39.46%), WIJ3_Sieved (11%) and IS2_Sieved (6.5%). The northern stations (RIJ) were dominated by monothalamiids assigned to Clade Y and Monothalamea_XXX. At the outermost station RIJ4, also higher percentages of *Psammophaga* sp. and *Psammosphaera* sp. sequences occurred. At the stations located at eastern Svalbard (NAL), the number of Clade Y sequences decreased towards the glacier-distant stations, while the percentage of Monothalamea_XXX increased. Also, glacier-distal stations were characterized by a higher proportion of Globothalamea, mainly *Reophax* sp. and *Stainforthia* sp. The foraminiferal community in EDG1 was dominated by a monothalamid *Psammosphaera* sp. (up to 90%), while *Hippocrepinella* sp. dominated in EDG2 and EDG3 (from 11% to 84%). Also, the percentage of *Reophax* sp. sequences increased towards the glacier-distal stations, reaching up to 34.68% at the station EDG3_Sieved.

355

356 ## 4.4. Alpha and beta diversity patterns

357 ### 4.4.1. Alpha diversity

358 The four alpha-diversity indices (Observed ASVs, Chao1, Simpson and Shannon) were
359 measured separately for sieved and unsieved datasets (Fig. 7) and showed clear variation
360 between different locations. On the one hand, the number of ASVs collected varied
361 substantially depending on sample treatments and locations. In terms of sample treatment,
362 sieved samples recovered higher Observed ASVs and Chao1 indices (Figs. 7a,b), but not
363 Simpson or Shannon (Figs. 7c,d). On the other hand, the measured alpha-diversity indices
364 tended to increase with increasing distance from the glacier (except station RIJ2). In general,
365 the alpha-diversity indices of the fjords (IS, WIJ, RIJ) were higher than those of open sea areas
366 (NAL, EDG), indicating higher foraminiferal diversity in fjords.

367

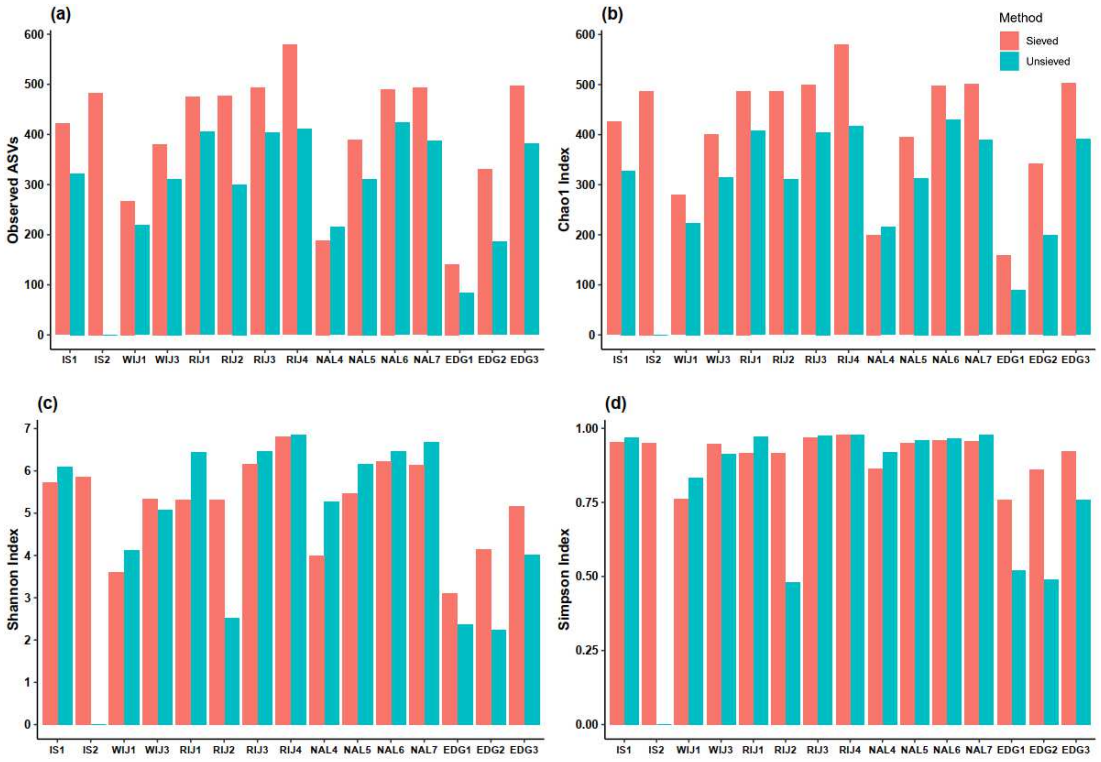

Figure 7. Bar plots of alpha diversity indices, including community richness (a: Observed ASVs, b: Chao1) and diversity (c: Shannon, d: Simpson) for the 15 sieved samples and 14 unsieved samples using retained ASV read abundances.

4.4.2. Beta diversity

The non-metric multidimensional scaling plots (nMDS) and heatmap of all stations (Fig. 8) supported the findings of the ordinances, showing that foraminiferal communities detected in the sieved samples differed from those detected in the unsieved samples, but not significantly (Table S7). The nMDS and heatmap patterns also revealed spatial distribution of the foraminiferal communities among the different localities. In Fig. 8a, the nMDS analyses produced a similar pattern with sieved and unsieved datasets, although community segregation was observed in ordinations of EDG and NAL sites. The communities were distinctly separated between fjord stations and opened sea stations, as shown by low-stress values. Although the fjord samples formed tight clusters, the samples from each fjord were not overlapping with the samples from other fjord locations. On the contrary, the communities obtained from EDG and NAL sites formed clusters with much larger internal compositional differences and has an overlap between the two sites. Heatmap further clarified the community structuration with the stations and datasets (Fig. 8b), which were not visible on the nMDS (except for NAL5). The sampling sites were grouped in two main clusters: cluster 1 aggregating 3 stations (EDG1, EDG2, NAL4) and cluster 2 comprising the 12 remaining stations that were grouped into three subclusters. The stations of two fjords (IS and WIJ) had homogeneous communities and formed one separate subcluster. Two other subclusters are formed by i) NAL6, NAL5, EDG3, and ii) all RIJ stations and NAL7.

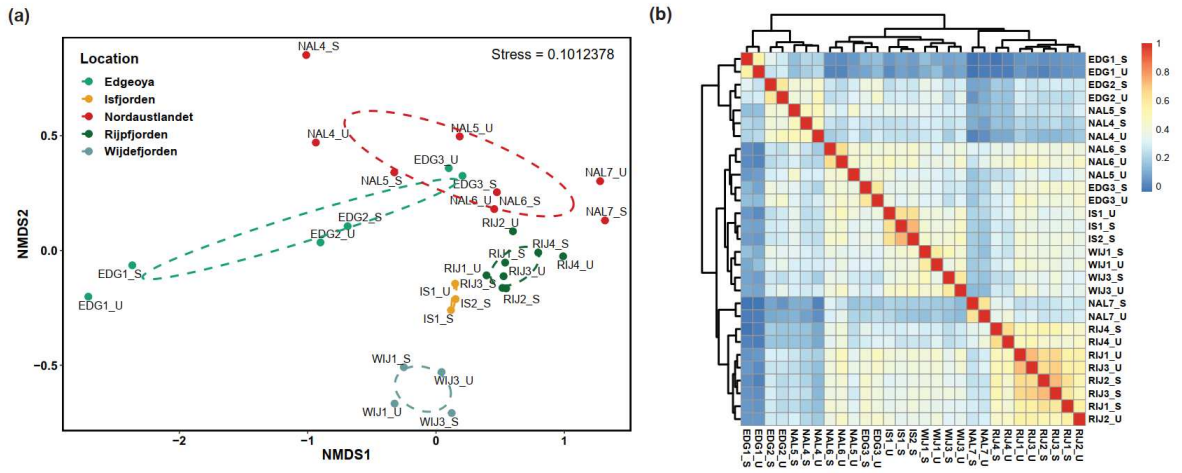

391

392 **Figure 8.** Community structuring of benthic foraminifera using nonlinear
393 multidimensional scaling based on Bray-Curtis distance similarity coefficient **(a)** and heatmap
394 based on Spearman's correlation coefficient for fractions and unsieved samples **(b).** Stress
395 value is displayed on the plot.

396

397 **4.4. sPLS Prediction Analysis**

398 In the results of the sPLS regression, we detected several foraminiferal ASVs lineages
399 for which relative sequence abundance correlated with environmental parameters (Fig. 9 and
400 Table S8). The sPLS regression and subsequent hierarchical clustering suggested that the data
401 was separated into three clusters (Fig. 9). These include lineages identified as potential
402 indicators of water mass characteristics.

403 In cluster I.A, the ASVs exhibited a positive correlation with turbidity and negative
404 correlation with factors such as depth, the salinity of bottom water and temperature of the
405 surface water, with the ASVs predominantly affiliated as members of monothalamiids:
406 *Hippocrepinella* sp. (ASV3, ASV10, ASV21), *Psammosphaera* sp. (ASV6), *Saccamminidae*
407 sp. (ASV12), CladeY_spallogJAP (ASV22), STICKY_ICE (ASV39), *Pelosinella fusiformis*
408 (ASV82), and globothalamids: *Buliminella* sp. (ASV14), *Nonionellina labradorica* (ASV20),
409 *Cibicides* sp. (ASV91). The ASVs within cluster II revealed a strong and positive correlation

with temperature as well as a negative correlation with salinity in the surface water masses. This cluster included globothalamids: *Stainforthia* sp. (ASV1), *Virgulinella fragilis* (ASV79), *Reophax sp.* (ASV92*), Cibicidoides fletcheri* (ASV23), and monothalamiids: *Psammophaga* sp. (ASV25, ASV34, ASV42, ASV53, ASV64), *Micrometula* sp. (ASV4), ENFOR2_EnvHabIC19 (ASV45), CladeA (ASV85, ASV32). Some ASVs belonging to cluster II also had a strong positive correlation with the depth and bottom water salinity (Table S8).

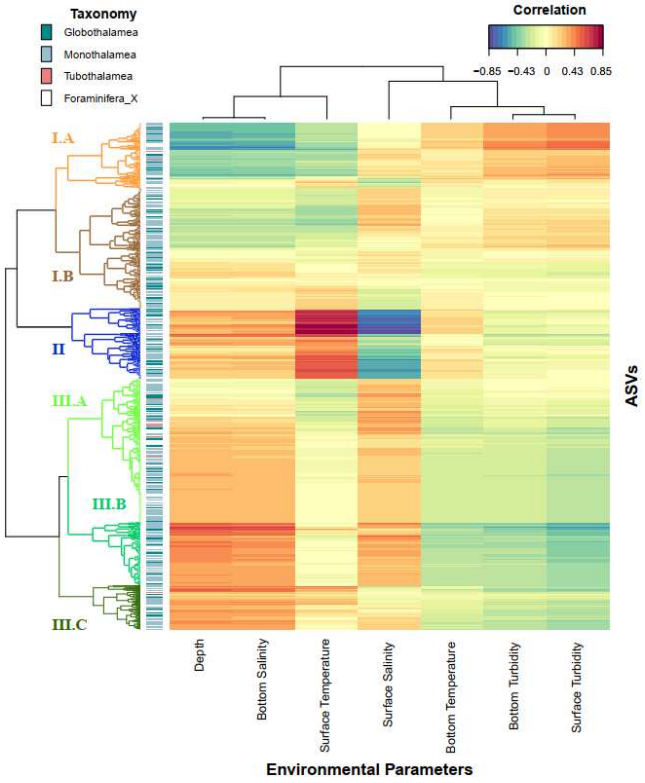

Figure 9. Clustered image map (CIM) of the first two sPLS dimensions, displaying pairwise correlations between foraminiferal ASVs of combined unsieved and sieved samples associated with environmental parameters. Correlations between ASVs and environmental parameters are depicted as a clustered heat map (detailed results in Table S8). Red and blue indicate positive and negative correlations, respectively.

Additionally, we observed positive correlations with depth and salinity in clusters III.A and III.B. Most of ASVs belonging to these clusters were classified as undetermined Monothalamea: Monothalamea_XX (39 ASVs), ENFOR XX (20 ASVs), CladeG (19 ASVs), CladeTIN (16 ASVs). In terms of ASV abundance, the dominant ASVs included environmental monothalamiids (ASV11, ASV44, ASV81, ASV66, ASV93, ASV88, ASV69, ASV78), CladeC_spsaccam (ASV59), *Gloiogullmia* sp. (ASV63), *Cibicides* sp. (ASV38), *Nonionella auris* (ASV31), rotalid (ASV96), *Reophax* sp. (ASV41, ASV13, ASV18), *Stainforthia* sp. (ASV77). Cluster III.C had positive associations with the depth, the bottom water salinity, and the surface temperature. ENFOR2_XXX (ASV408, ASV136, ASV125) exhibited their highest abundances of this cluster.

5. Discussion

5.1. Is pre-sieving useful for foraminiferal metabarcoding?

The methodological aim of this study was to compare the results of metabarcoding analyses based on sieved and unsieved sediment samples. Sieving is a common procedure in the conventional microscopic study of foraminiferal assemblage analyzing mainly hard-shelled, multi-chambered taxa preserved in fixed and dried sediment samples [78]. In contrast, metabarcoding studies of unsieved sediment samples usually provide a foraminiferal assemblage dominated by poorly known, soft-shelled or naked monothalamous taxa [37,41]. Because of this, it is difficult to compare the results of traditional morphology-based studies with those of metabarcoding analysis, which provide very different types of data [35].

As shown by our study, the taxonomic composition of different size fractions is not the same. For example, the order Rotaliida was the most abundant in 500-100 µm and 100-63 µm size fractions. Also, another hard-shelled order Textulariida, which is microscopically studied in the 500-100 µm fraction, in metabarcoding data is present mainly in fractions 500-100 µm

449 and 100-63 µm (Fig. 5c) This is congruent with the rotaliids and textulariids dominating
450 microscopic assemblage found in >63 µm sieved fraction. On the other hand, the smallest
451 fraction (<63 µm) was dominated by monothalamiids and undetermined Foraminifera (Fig.
452 5C), which may suggest the presence of some genetically unknown, tiny monothalamous
453 species.

454 We also observed some differences between sieved and unsieved samples regarding the
455 alpha diversity. The total number of recovered ASVs was clearly higher in sieved than in
456 unsieved samples (approximately 30% ASVs). However, this could be explained by the
457 difference in the number of DNA extractions, PCR amplifications, and sequencing depth. In
458 the case of sieved samples, the datasets included four DNA extractions, one for each size
459 fraction, while only one DNA extraction was performed for non-sieved sediment samples. In
460 total, the number of sequences obtained for sieved fractions was several times higher, allowing
461 to detection of more diversity in sieved compared to unsieved samples. However, no significant
462 difference between the sieved/unsieved samples was observed in alpha-diversity measures such
463 as Shannon's and Simpson's that take abundance and evenness of the sample into consideration
464 as shown in Fig. 7. Although sieving might have been predicted to lead to a reduction in alpha
465 diversity due to the loss of microfauna and extracellular debris, this has not been observed in
466 previous studies [79,80]. In addition, NMDS of the beta-diversity matrices and correlation test
467 showed sieved and unsieved samples clustered together (Fig. 8, Table S7), indicating that there
468 is no significant difference in community composition inferred by the two methods.

469 To conclude, the decision of whether the sediment samples should be sieved or not shall
470 be based on the type of questions one wants to answer with metabarcoding data as well as the
471 composition and characteristics of initial samples. Sieving procedure combined with
472 metabarcoding analysis might be useful if targeted at particular groups of foraminifera (e.g.,
473 Rotaliida, Textulariida), for example, to compare with microscopic studies or to identify some

474 tiny species present in fine size fractions. In general, the unsieved samples provide a more
475 complete overview of the taxonomic composition of the foraminiferal community. However,
476 as shown by our study, both metabarcoding datasets reveal similar trends in foraminiferal
477 diversity. Size-sieving might have some advantages, however, it also has some drawbacks, as
478 (i) it is time-consuming, (ii) requires higher volume samples, and (iii) there is a possibility of
479 cross-contamination between samples. Therefore, either extracting DNA directly from
480 sediment or after sieving should be carefully considered when evaluating foraminiferal
481 communities across metabarcoding studies.
482
483 **5.2. Distribution patterns of foraminifera in Svalbard**
484 The most striking result of this study is the variations of foraminiferal assemblage
485 between different sampling localities. Although, there are some similar trends documented by
486 diversity indices at different locations, such as the proportion of monothalamiids in near-glacier
487 settings (Fig. 6), or the increase of alpha diversity from glacier proximal/inner to glacier-
488 distant/outer stations (Fig. 7), which are in agreement with the previous morphology-based
489 studies [81-83], the composition of foraminiferal communities is generally specific to each
490 location. Each fjord forms a separate cluster and only some stations at open-water areas overlap
491 with each other (Fig. 8a).
492 The high-Arctic settings are usually considered as a cold system influenced at different
493 levels by ArW during summer to late autumn [84], and covered by sea ice in winter [9,59,85].
494 However, the increased influence of AW and winter sea-ice loss is observed in recent years
495 [10,86,87]. We speculate that hydrographic conditions would lead to isolating populations from
496 different settings and creating unique structures of the foraminiferal community.
497 It is well known that the unique habitats of fjords can support a high diversity and
498 distinct biological communities [81-83,88-90]. Fjords create a variety of habitats suitable for specific

499 species, where many species can converge and reach high population densities. Western
500 Spitsbergen fjords are among the most AW-impacted areas. Both Isfjorden and Wijdefjorden
501 are directly connected to the slope and shelf areas, which enables AW penetration into the
502 fjords. Moreover, Isfjorden stations are located in the central basin of the fjord, which resulted
503 in limited glacial influence. This led to the formation of foraminifera communities
504 characterized by a relatively high proportion of globothalamids and the presence of
505 monothalamiids community dominated by the genera *Psammophaga* and *Micrometula* (Fig.
506 6). Similar distribution patterns were previously observed in west Spitsbergen fjords [81,82]. Only
507 station WIJ1 displayed a unique structure with a clear dominance of Rotaliida (Figs. 4 and 6).
508 Station WIJ1 is located in the inner fjord, close to the glacier termini and is influenced by turbid
509 meltwater runoffs. The dominance of Rotaliida contradicts previous studies, indicating that
510 glacier proximal settings are dominated by monothalamous foraminifera [81,91]. However, this
511 distribution pattern could be also explained by the natural patchiness of foraminiferal
512 distribution.

513 In the northern site (RIJ), the dominant component of foraminiferal assemblages were
514 undetermined monothalamiids (Figs 4 and 6). The dominance of these undetermined, small,
515 soft-walled species was previously observed in areas characterized by a high level of
516 environmental disturbance [42,81]. Northern Svalbard in general and Rijpfjorden in particular, are
517 considered to be a typical Arctic setting, where sea ice forms in autumn and lasts until summer.
518 Also, the drifting ice pack is often transported to the fjord during the summer [59]. Forming of
519 sea ice is associated with brine rejection. Cold and dense brines sink to the bottom, which leads
520 to the formation of cold and saline WCW. This process may create a more severe environment
521 where monothalamiids thrive.

522 Foraminiferal communities of open water areas (eastern Svalbard) have generally lower
523 diversity and form different groups compared to those from western Svalbard fjords. Stations

524 from the regions of Nordaustlandet and Edgeøya are located in front of large tidewater glaciers,
525 releasing large amounts of turbid meltwater (Fig. S1). However, only Nordaustlandet was
526 influenced by AW and TAW, while the Edgeøya oceanographic conditions were shaped mainly
527 by local water masses. These led to the creation of distinctly different foraminiferal
528 communities. NAL stations were characterized by a wide range of undetermined
529 monothalamiids, while the EDG stations were dominated by a few monothalamous species
530 representing genera *Hipocrepinella* and *Psammosphaera* (Fig. 6). In particular, station EDG1
531 exhibited a unique foraminiferal community, composed almost exclusively of *Psammosphaera*
532 sp. Psammosphaerids were previously recorded in Spitsbergen fjords [82,90] and also in deep-sea
533 areas affected by bottom currents [92]. Environmental conditions at station EDG1 are probably
534 the most dynamic and severe among the studied stations, as the large sub-bottom meltwater
535 outflow was recorded (Fig. S1).
536
537 **5.3. Influence of atlantification on foraminifera community**
538 The response of benthic foraminifera to alterations in temperature and salinity in the
539 water column are common and include expansions or retractions of distribution ranges or
540 changes in assemblage compositions [93-95]. We hypothesize that the composition of
541 foraminiferal communities in our data resulted from water mass conditions. This hypothesis is
542 strengthened by the clear clustering of the community in groups corresponding to different
543 oceanographic regimes, in which stations from regions impacted by AW and/or sea-ice
544 clustered separately.
545 As shown by the nMDS plot and heatmap (Fig. 8), the separation between two main
546 clusters has a strong relationship with characteristics of water masses. Cluster 1 comprises
547 exclusively the stations of the eastern part of the archipelago (EDG1, EGD2, NAL4, NAL5),
548 characterized by colder, and less salty water, associated with turbid glacial meltwater [96]. On

549 the contrary, Cluster 2 includes mainly stations from the western and northern part of Svalbard
550 where the impact of warmer and more saline Atlantic Water (AW) was much pronounced,
551 confirmed by our CTD profile (Fig. 2). Also, sub-clusters that formed within cluster 2 reflected
552 different impacts of AW. The first sub-cluster comprises stations located in the glacial-distant
553 regions of Nordaustlandet and Edgeøya, influenced mainly by TAW. The second sub-cluster
554 includes the most AW-impacted stations located on the western coast of the archipelago, while
555 the third sub-cluster is composed of stations located in north-eastern Svalbard, influenced both
556 by the inflow of AW and sea-ice.

557 The increased AW inflow, higher light availability, and the decline of sea-ice around
558 Svalbard affect the primary productivity, changing both the timing of phytoplankton bloom
559 and phytoplankton community structure. This may have significant effects on food web
560 dynamics, affecting higher trophic levels, including benthic communities [97]. On the other hand,
561 recent model projections indicated low mean habitat loss of benthic macrofauna under recent
562 climate changes, which questions the vulnerability of Arctic benthos to atlantification [98]. This
563 stands in clear opposition to the morphological observations that testate foraminifera
564 communities from Svalbard fjords revealed significant changes, both in terms of abundance
565 and species composition, related to atlantification [99]. Our study confirms the impact of AW on
566 foraminiferal communities, suggesting that AW is one of the primary factors shaping the
567 benthic foraminifera assemblages and thus foraminifera may be potential indicators of
568 atlantification.

569 Through sPLS analysis of combining datasets, we identified foraminiferal taxa that
570 could become potential bioindicators of “atlantification”. This group of species includes some
571 monothalamiids belonging to genera *Psammophaga* and *Micrometula* as well as some
572 undetermined monothalamous species belonging to environmental lineage ENFOR2 and Clade
573 A. The genera *Psammophaga* and *Micrometula* are widespread in many coastal areas including

polar regions [100,101] and are considered as bioindicator candidates in several studies [37,102]. However, the limited knowledge about the ecology of those taxa, as well as lack of reference database of their distribution in the North Atlantic region precludes making any general conclusions. Among potential bioindicators, there are also some globothalamids, such as *Stainforthia* sp., *Virgulinella fragilis*, *Reophax* sp., and *Cibicidoides fletcheri*. *Cibicidoides* species is common in the North Atlantic [103], but to the best of our knowledge, it was not recorded in Svalbard before. One of the major signs of atlantification is the northward shift of boreal species, the trend observed in the case of zooplankton, fish, and benthic organisms [97]. A recent morphological study of Svalbard foraminifera revealed the presence of boreal species *Melonis affinis* in the northern part of the archipelago [99]. *Reophax* sp. and, *Stainforthia* sp. are commonly found in Svalbard [83]. Also, species belonging to the genus *Reophax* are considered as indicators of AW [104]. The agreement of our results with previous morphology-based studies further proves the potential of foraminifera in biomonitoring studies.

Apart from indicators of atlantification, we identified monothalamiids that show a strong correlation with turbidity, but not with depth or salinity. These species included *Hippocrepinella* sp., *Psammosphaera* sp., *Saccamminidae* sp., CladeY_spallogJAP, and several unassigned STICKY_ICE ASVs. This correlation is particularly strong in stations closer to the coast, which is probably caused by enhanced turbidity due to sediment-laden meltwater plumes. *Hippocrepinella* sp., *Psammosphaera* sp., *Saccamminidae* sp., as well as monothalamiids belonging to Clade Y were previously recorded in Svalbard [82,90,91]. Clade Y comprises mainly undetermined monothalamiids, known from environmental sequencing. They were abundantly sequenced in the settings characterized by a high level of environmental disturbance, suggesting that they are highly resistant to environmental disturbance [37]. Moreover, morphological studies reported *Hippocrepinella* sp., *Psammosphaera* sp., *Saccamminidae* sp., in the shallow-water parts of the fjords, located close to meltwater

outflows [81,82,90]. These findings underline how important can be to include soft-shelled monothalamous foraminifera in metabarcoding studies to enhance limited knowledge about their ecology for potential use in biomonitoring.

6. Conclusions

This study is the first to use high-throughput sequencing to comprehensively analyze the foraminiferal communities within marine sediments from Svalbard, which helps to provide more knowledge of foraminiferal diversity and distribution patterns in the Arctic's fjords. The DNA sequencing results from sieved and unsieved sediment revealed a high diversity of the Svalbard foraminifera compared to traditional morphology-based studies and variation in the taxonomic composition of foraminiferal communities from five sampling areas. Foraminiferal diversity and species richness increased from glacier proximal/inner to glacier-distant/outer stations and were higher in the fjords than in the open water. Moreover, the structure of foraminiferal community is clearly influenced by different water masses, with a particular impact of Atlantic Water in the Svalbard region. Numerous potential molecular foraminiferal bioindicators for atlantification were identified. This should be confirmed by analysing many more samples from reference areas in North Atlantic. With the increasing numbers of metabarcoding studies, the impact of atlantification on Arctic benthic communities identified in this study could be better assessed and expanded to those organisms that are not covered by the conventional morphological approach.

Acknowledgements

The research leading to these results has been funded by Norwegian Financial Mechanism for 2014-2021, project no 2019/34/H/ST10/00682. Jan P and IBA were supported by the Swiss

National Science Foundation grant 31003A_179125. Joanna P was also supported by the grant no. 2018/31/B/ST10/01616 funded by the National Science Centre in Poland. We express our thanks to the captain and crew of the R/V Oceania.

Authors contributions

N-LN, Joanna P, Jan P and MZ conceived the idea for the study and developed the research methodology; Joanna P and MZ collected the samples and performed laboratory analysis; N-LN produced the dataset; N-LN and Joanna. P performed the bioinformatic analyses and wrote the manuscript with contributions and comments from all co-authors. All authors reviewed and approved the final manuscript.

Declaration of Competing Interest

The authors declare no competing interests.

References

1 Beszczynska-Möller, A., Fahrbach, E., Schauer, U. & Hansen, E. Variability in Atlantic water temperature and transport at the entrance to the Arctic Ocean, 1997–2010. *ICES Journal of Marine Science* **69**, 852-863, doi:10.1093/icesjms/fss056 (2012).

2 Polyakov, I. V. *et al.* Greater role for Atlantic inflows on sea-ice loss in the Eurasian Basin of the Arctic Ocean. *Science* **356**, 285-291, doi:10.1126/science.aai8204 (2017).

3 Onarheim, I. H., Smedsrud, L. H., Ingvaldsen, R. B. & Nilsen, F. Loss of sea ice during winter north of Svalbard. *Tellus A: Dynamic Meteorology and Oceanography* **66**, 23933, doi:10.3402/tellusa.v66.23933 (2014).

4 Berge, J., Johnsen, G., Nilsen, F., Gulliksen, B. & Slagstad, D. Ocean temperature oscillations enable reappearance of blue mussels Mytilus edulis in Svalbard after a 1000 year absence. *Marine Ecology Progress Series* **303**, 167-175 (2005).

5 Slagstad, D., Ellingsen, I. H. & Wassmann, P. Evaluating primary and secondary production in an Arctic Ocean void of summer sea ice: An experimental simulation approach. *Prog Oceanogr* **90**, 117-131, doi:https://doi.org/10.1016/j.pocean.2011.02.009 (2011).

6 Zajączkowski, M., Nygård, H., Hegseth, E. N. & Berge, J. Vertical flux of particulate matter in an Arctic fjord: the case of lack of the sea-ice cover in Adventfjorden 2006–2007. *Polar Biology* **33**, 223-239, doi:10.1007/s00300-009-0699-x (2010).

7 Kortsch, S., Primicerio, R., Fossheim, M., Dolgov, A. V. & Aschan, M. Climate change alters the structure of arctic marine food webs due to poleward shifts of boreal generalists. *Proceedings of the Royal Society B: Biological Sciences* **282**, 20151546, doi:doi:10.1098/rspb.2015.1546 (2015).

8 Serreze, M. C. & Barry, R. G. Processes and impacts of Arctic amplification: A research synthesis. *Global and Planetary Change* **77**, 85-96, doi:https://doi.org/10.1016/j.gloplacha.2011.03.004 (2011).

9 Dai, A., Luo, D., Song, M. & Liu, J. Arctic amplification is caused by sea-ice loss under increasing CO2. *Nat Commun* **10**, 121, doi:10.1038/s41467-018-07954-9 (2019).

10 Nilsen, F., Cottier, F., Skogseth, R. & Mattsson, S. Fjord–shelf exchanges controlled by ice and brine production: The interannual variation of Atlantic Water in Isfjorden,

Svalbard. *Continental Shelf Research* **28**, 1838-1853, doi:https://doi.org/10.1016/j.csr.2008.04.015 (2008).

11 Vihtakari, M. *et al.* Black-legged kittiwakes as messengers of Atlantification in the Arctic. *Sci Rep* **8**, 1178, doi:10.1038/s41598-017-19118-8 (2018).

12 Descamps, S. *et al.* Climate change impacts on wildlife in a High Arctic archipelago - Svalbard, Norway. *Glob Chang Biol* **23**, 490-502, doi:10.1111/gcb.13381 (2017).

13 Frainer, A. *et al.* Climate-driven changes in functional biogeography of Arctic marine fish communities. *Proc Natl Acad Sci U S A* **114**, 12202-12207, doi:10.1073/pnas.1706080114 (2017).

14 Fossheim, M. *et al.* Recent warming leads to a rapid borealization of fish communities in the Arctic. *Nature Climate Change* **5**, 673-+ (2015).

15 Weydmann-Zwolicka, A. *et al.* Zooplankton and sediment fluxes in two contrasting fjords reveal Atlantification of the Arctic. *Sci Total Environ* **773**, 145599, doi:10.1016/j.scitotenv.2021.145599 (2021).

16 Hop, H. *et al.* Pelagic Ecosystem Characteristics Across the Atlantic Water Boundary Current From Rijpfjorden, Svalbard, to the Arctic Ocean During Summer (2010–2014). *Frontiers in Marine Science* **6**, doi:10.3389/fmars.2019.00181 (2019).

17 Grabowski, M. *et al.* Contrasting molecular diversity and demography patterns in two intertidal amphipod crustaceans reflect Atlantification of High Arctic. *Marine Biology* **166**, 155, doi:10.1007/s00227-019-3603-4 (2019).

18 Barton, A. D., Irwin, A. J., Finkel, Z. V. & Stock, C. A. Anthropogenic climate change drives shift and shuffle in North Atlantic phytoplankton communities. *Proc Natl Acad Sci U S A* **113**, 2964-2969, doi:10.1073/pnas.1519080113 (2016).

19 Neukermans, G., Oziel, L. & Babin, M. Increased intrusion of warming Atlantic water leads to rapid expansion of temperate phytoplankton in the Arctic. *Glob Chang Biol* **24**, 2545-2553, doi:10.1111/gcb.14075 (2018).

20 Meilland, J. *et al.* Population dynamics of modern planktonic foraminifera in the western Barents Sea. *Biogeosciences* **17**, 1437-1450, doi:10.5194/bg-17-1437-2020 (2020).

21 Ofstad, S. *et al.* Shell density of planktonic foraminifera and pteropod species Limacina helicina in the Barents Sea: Relation to ontogeny and water chemistry. *PLoS One* **16**, e0249178, doi:10.1371/journal.pone.0249178 (2021).

22 Schoenle, A. *et al.* High and specific diversity of protists in the deep-sea basins dominated by diplonemids, kinetoplastids, ciliates and foraminiferans. *Commun Biol* **4**, 501, doi:10.1038/s42003-021-02012-5 (2021).

23 Gooday, A. J. & Jorissen, F. J. Benthic foraminiferal biogeography: controls on global distribution patterns in deep-water settings. *Ann Rev Mar Sci* **4**, 237-262, doi:10.1146/annurev-marine-120709-142737 (2012).

24 Murray, J. W. *Ecology and Applications of Benthic Foraminifera*. (Cambridge University Press, 2006).

25 Kawahata, H. *et al.* Perspective on the response of marine calcifiers to global warming and ocean acidification—Behavior of corals and foraminifera in a high CO2 world “hot house”. *Progress in Earth and Planetary Science* **6**, 5, doi:10.1186/s40645-018-0239-9 (2019).

26 Wittmann, A. C. & Pörtner, H.-O. Sensitivities of extant animal taxa to ocean acidification. *Nature Climate Change* **3**, 995-1001, doi:10.1038/nclimate1982 (2013).

27 Prazeres, M., Roberts, T. E. & Pandolfi, J. M. Variation in sensitivity of large benthic Foraminifera to the combined effects of ocean warming and local impacts. *Scientific Reports* **7**, 45227, doi:10.1038/srep45227 (2017).

28 Bohmann, K. *et al.* Environmental DNA for wildlife biology and biodiversity monitoring. *Trends Ecol Evol* **29**, 358-367, doi:10.1016/j.tree.2014.04.003 (2014).

29 Holman, L. E. *et al.* Animals, protists and bacteria share marine biogeographic patterns. *Nature Ecology & Evolution* **5**, 738-746, doi:10.1038/s41559-021-01439-7 (2021).

30 Pawlowski, J., Bonin, A., Boyer, F., Cordier, T. & Taberlet, P. Environmental DNA for biomonitoring. *Molecular Ecology* **30**, 2931-2936, doi:https://doi.org/10.1111/mec.16023 (2021).

31 Lejzerowicz, F., Esling, P. & Pawlowski, J. Patchiness of deep-sea benthic Foraminifera across the Southern Ocean: Insights from high-throughput DNA sequencing. *Deep Sea Research Part II: Topical Studies in Oceanography* **108**, 17-26, doi:https://doi.org/10.1016/j.dsr2.2014.07.018 (2014).

32 Pawlowski, J. & Lecroq, B. Short rDNA barcodes for species identification in foraminifera. *J Eukaryot Microbiol* **57**, 197-205, doi:10.1111/j.1550-7408.2009.00468.x (2010).

33 Armbrecht, L. H. *et al.* Ancient DNA from marine sediments: Precautions and considerations for seafloor coring, sample handling and data generation. *Earth-Science Reviews* **196**, 102887, doi:https://doi.org/10.1016/j.earscirev.2019.102887 (2019).

34 Vargas, C. d. *et al.* Eukaryotic plankton diversity in the sunlit ocean. *Science* **348**, 1261605, doi:doi:10.1126/science.1261605 (2015).

35 Frontalini, F. *et al.* Benthic foraminiferal metabarcoding and morphology-based assessment around three offshore gas platforms: Congruence and complementarity. *Environ Int* **144**, 106049, doi:10.1016/j.envint.2020.106049 (2020).

36 Pawlowski, J. *et al.* Benthic monitoring of salmon farms in Norway using foraminiferal metabarcoding. *Aquacult Env Interac* **8**, 371-386 (2016).

37 Pawlowski, J., Esling, P., Lejzerowicz, F., Cedhagen, T. & Wilding, T. A. Environmental monitoring through protist next-generation sequencing metabarcoding: assessing the impact of fish farming on benthic foraminifera communities. *Molecular Ecology Resources* **14**, 1129-1140 (2014).

38 Chronopoulou, P. M., Salonen, I., Bird, C., Reichart, G. J. & Koho, K. A. Metabarcoding Insights Into the Trophic Behavior and Identity of Intertidal Benthic Foraminifera. *Frontiers in microbiology* **10**, 1169, doi:10.3389/fmicb.2019.01169 (2019).

39 Cordier, T., Barrenechea, I., Lejzerowicz, F., Reo, E. & Pawlowski, J. Benthic foraminiferal DNA metabarcodes significantly vary along a gradient from abyssal to hadal depths and between each side of the Kuril-Kamchatka trench. *Prog Oceanogr* **178** (2019).

40 Lejzerowicz, F. *et al.* Eukaryotic Biodiversity and Spatial Patterns in the Clarion-Clipperton Zone and Other Abyssal Regions: Insights From Sediment DNA and RNA Metabarcoding. *Frontiers in Marine Science* **8**, doi:10.3389/fmars.2021.671033 (2021).

41 Lecroq, B. *et al.* Ultra-deep sequencing of foraminiferal microbarcodes unveils hidden richness of early monothalamous lineages in deep-sea sediments. *Proc Natl Acad Sci U S A* **108**, 13177-13182, doi:10.1073/pnas.1018426108 (2011).

764 42 Pawlowska, J. *et al.* Ancient DNA sheds new light on the Svalbard foraminiferal
765 fossil record of the last millennium. *Geobiology* **12**, 277-288, doi:10.1111/gbi.12087
766 (2014).
767 43 Pawlowska, J., Wollenburg, J. E., Zajaczkowski, M. & Pawlowski, J. Planktonic
768 foraminifera genomic variations reflect paleoceanographic changes in the Arctic:
769 evidence from sedimentary ancient DNA. *Sci Rep* **10**, 15102, doi:10.1038/s41598-
770 020-72146-9 (2020).
771 44 Barrenechea Angeles, I. *et al.* Planktonic foraminifera eDNA signature deposited on
772 the seafloor remains preserved after burial in marine sediments. *Sci Rep* **10**, 20351,
773 doi:10.1038/s41598-020-77179-8 (2020).
774 45 Elbrecht, V., Peinert, B. & Leese, F. Sorting things out: Assessing effects of unequal
775 specimen biomass on DNA metabarcoding. *Ecol Evol* **7**, 6918-6926,
776 doi:10.1002/ece3.3192 (2017).
777 46 Leray, M. & Knowlton, N. DNA barcoding and metabarcoding of standardized
778 samples reveal patterns of marine benthic diversity. *P Natl Acad Sci USA* **112**, 2076-
779 2081 (2015).
780 47 Brandt, M. I. *et al.* Evaluating sediment and water sampling methods for the
781 estimation of deep-sea biodiversity using environmental DNA. *Sci Rep* **11**, 7856,
782 doi:10.1038/s41598-021-86396-8 (2021).
783 48 Sinniger, F. *et al.* Worldwide Analysis of Sedimentary DNA Reveals Major Gaps in
784 Taxonomic Knowledge of Deep-Sea Benthos. *Frontiers in Marine Science* **3**,
785 doi:10.3389/fmars.2016.00092 (2016).
786 49 Cottier, F. *et al.* Water mass modification in an Arctic fjord through cross-shelf
787 exchange: The seasonal hydrography of Kongsfjorden, Svalbard. *Journal of*

Geophysical Research: Oceans **110**, doi:https://doi.org/10.1029/2004JC002757 (2005).

50 Blindheim, J. & Østerhus, S. in *The Nordic Seas: An Integrated Perspective* 11-37 (2005).

51 Loeng, H. Features of the physical oceanographic conditions of the Barents Sea. *Polar Research* **10**, 5-18, doi:https://doi.org/10.1111/j.1751-8369.1991.tb00630.x (1991).

52 Spielhagen, R. F. *et al.* Enhanced Modern Heat Transfer to the Arctic by Warm Atlantic Water. *Science* **331**, 450-453, doi:doi:10.1126/science.1197397 (2011).

53 Saloranta, T. M. & Haugan, P. M. Northward cooling and freshening of the warm core of the West Spitsbergen Current. *Polar Research* **23**, 79-88, doi:10.3402/polar.v23i1.6268 (2004).

54 Aagaard, K., Foldvik, A. & Hillman, S. R. The West Spitsbergen Current: Disposition and water mass transformation. *Journal of Geophysical Research: Oceans* **92**, 3778-3784, doi:https://doi.org/10.1029/JC092iC04p03778 (1987).

55 Bourke, R. H., Weigel, A. M. & Paquette, R. G. The westward turning branch of the West Spitsbergen Current. *Journal of Geophysical Research: Oceans* **93**, 14065-14077, doi:https://doi.org/10.1029/JC093iC11p14065 (1988).

56 Sternal, B. *et al.* Postglacial variability in near-bottom current speed on the continental shelf off south-west Spitsbergen. *Journal of Quaternary Science* **29**, 767–777, doi:10.1002/jqs.2748 (2014).

57 Nilsen, F., Skogseth, R., Vaardal-Lunde, J. & Inall, M. A Simple Shelf Circulation Model: Intrusion of Atlantic Water on the West Spitsbergen Shelf. *Journal of Physical Oceanography* **46**, 1209-1230, doi:10.1175/jpo-d-15-0058.1 (2016).

58 Kowalewski, W., Rudowski, S. & Zalewski, S. M. Seismoacoustic studies within Wijdefjorden, Spitsbergen. *Polish Polar Research* **vol. 11**, 287-300-287-300 (1990).

59 Ambrose Jr., W. G., Carroll, M. L., Greenacre, M., Thorrold, S. R. & McMahon, K. W. Variation in Serripes groenlandicus (Bivalvia) growth in a Norwegian high-Arctic fjord: evidence for local- and large-scale climatic forcing. *Global Change Biology* **12**, 1595-1607, doi:https://doi.org/10.1111/j.1365-2486.2006.01181.x (2006).

60 Dowdeswell, J. A. *et al.* Digital Mapping of the Nordaustlandet Ice Caps from Airborne Geophysical Investigations. *Annals of Glaciology* **8**, 51-58, doi:10.3189/S0260305500001130 (1986).

61 Dowdeswell, J. A. & Bamber, J. L. On the glaciology of Edgeøya and Barentsøya, Svalbard. *Polar Research* **14**, 105-122, doi:10.3402/polar.v14i2.6658 (1995).

62 Knies, J., Brookes, S. & Schubert, C. J. Re-assessing the nitrogen signal in continental margin sediments: New insights from the high northern latitudes. *Earth Planet Sc Lett* **253**, 471-484 (2007).

63 Dufresne, Y., Lejzerowicz, F., Perret-Gentil, L. A., Pawlowski, J. & Cordier, T. SLIM: a flexible web application for the reproducible processing of environmental DNA metabarcoding data. *BMC Bioinformatics* **20**, 88, doi:10.1186/s12859-019-2663-2 (2019).

64 Callahan, B. J. *et al.* DADA2: High-resolution sample inference from Illumina amplicon data. *Nat Methods* **13**, 581-583, doi:10.1038/nmeth.3869 (2016).

65 Pawłowska, J., Pawlowski, J. & Zajączkowski, M. Dataset of foraminiferal sedimentary DNA (sedDNA) sequences from Svalbard. *Data in Brief* **30**, 105553, doi:https://doi.org/10.1016/j.dib.2020.105553 (2020).

66 Froslev, T. G. *et al.* Algorithm for post-clustering curation of DNA amplicon data yields reliable biodiversity estimates. *Nat Commun* **8**, 1188, doi:10.1038/s41467-017-01312-x (2017).

67 Holzmann, M. & Pawlowski, J. An updated classification of rotaliid foraminifera based on ribosomal DNA phylogeny. *Marine Micropaleontology* **132**, 18-34, doi:https://doi.org/10.1016/j.marmicro.2017.04.002 (2017).

68 Pawlowski, J., Holzmann, M. & Tyszka, J. New supraordinal classification of Foraminifera: Molecules meet morphology. *Marine Micropaleontology* **100**, 1-10, doi:https://doi.org/10.1016/j.marmicro.2013.04.002 (2013).

69 Guillou, L. *et al.* The Protist Ribosomal Reference database (PR2): a catalog of unicellular eukaryote small sub-unit rRNA sequences with curated taxonomy. *Nucleic Acids Res* **41**, D597-604, doi:10.1093/nar/gks1160 (2013).

70 Altschul, S. F., Gish, W., Miller, W., Myers, E. W. & Lipman, D. J. Basic local alignment search tool. *Journal of Molecular Biology* **215**, 403-410, doi:https://doi.org/10.1016/S0022-2836(05)80360-2 (1990).

71 R Core Team. *R: A language and environment for statistical computing. R Foundation for Statistical Computing, Vienna, Austria, Available online at https://www.R-project.org/.* 2018).

72 Dusa, A. *venn: Draw Venn Diagrams*, <https://cran.r-project.org/web/packages/venn/venn.pdf> (2018).

73 Hsieh, T. C., Ma, K. H. & Chao, A. iNEXT: an R package for rarefaction and extrapolation of species diversity (Hill numbers). *Methods in Ecology and Evolution* **7**, 1451-1456, doi:https://doi.org/10.1111/2041-210X.12613 (2016).

74 Oksanen, J. A. I.

75 Kolde, R. Pretty Heatmaps. (2019).

76 Rohart, F., Gautier, B., Singh, A. & Le Cao, K. A. mixOmics: An R package for 'omics feature selection and multiple data integration. *PLoS Comput Biol* **13**, e1005752, doi:10.1371/journal.pcbi.1005752 (2017).

77 Le Cao, K. A., Rossouw, D., Robert-Granie, C. & Besse, P. A sparse PLS for variable selection when integrating omics data. *Stat Appl Genet Mol Biol* **7**, Article 35, doi:10.2202/1544-6115.1390 (2008).

78 Schönfeld, J. *et al.* The FOBIMO (FOraminiferal BIo-MOnitoring) initiative - Towards a standardised protocol for soft-bottom benthic foraminiferal monitoring studies. *Marine Micropaleontology* **94-95**, 1-13, doi:https://doi.org/10.1016/j.marmicro.2012.06.001 (2012).

79 Brannock, P. M. & Halanych, K. M. Meiofaunal community analysis by high-throughput sequencing: Comparison of extraction, quality filtering, and clustering methods. *Marine Genomics* **23**, 67-75, doi:https://doi.org/10.1016/j.margen.2015.05.007 (2015).

80 He, X., Sutherland, T. F. & Abbott, C. L. Improved efficiency in eDNA metabarcoding of benthic metazoans by sieving sediments prior to DNA extraction. *Environmental DNA* **n/a**, doi:https://doi.org/10.1002/edn3.172 (2020).

81 Sabbatini, A., Morigi, C., Negri, A. & Gooday, A. Distribution and biodiversity of stained monothalamous foraminifera from Tempelfjord, Svalbard. *Journal of Foraminiferal Research* **37**, 93-106, doi:10.2113/gsjfr.37.2.93 (2007).

82 Majewski, W., Pawłowski, J. & Zajączkowski, M. Monothalamous foraminifera from West Spitsbergen fjords, Svalbard: a brief overview. *Polish Polar Research* **vol. 26**, 269-285-269-285 (2005).

83 Hald, M. & Korsun, S. Distribution of modern benthic foraminifera from fjords of Svalbard, European Arctic. *Journal of Foraminiferal Research - J FORAMIN RES* **27**, 101-122, doi:10.2113/gsjfr.27.2.101 (1997).

84 Wallace, M. I. *et al.* Comparison of zooplankton vertical migration in an ice-free and a seasonally ice-covered Arctic fjord: An insight into the influence of sea ice cover on zooplankton behavior. *Limnology and Oceanography* **55**, 831-845, doi:https://doi.org/10.4319/lo.2010.55.2.0831 (2010).

85 Leu, E., Søreide, J. E., Hessen, D. O., Falk-Petersen, S. & Berge, J. Consequences of changing sea-ice cover for primary and secondary producers in the European Arctic shelf seas: Timing, quantity, and quality. *Prog Oceanogr* **90**, 18-32, doi:https://doi.org/10.1016/j.pocean.2011.02.004 (2011).

86 Dahlke, S. *et al.* The observed recent surface air temperature development across Svalbard and concurring footprints in local sea ice cover. *International Journal of Climatology* **40**, 5246-5265, doi:https://doi.org/10.1002/joc.6517 (2020).

87 Pavlova, O., Gerland, S. & Hop, H. in *The Ecosystem of Kongsfjorden, Svalbard* (eds Haakon Hop & Christian Wiencke) 105-136 (Springer International Publishing, 2019).

88 Walseng, B. *et al.* Freshwater diversity in Svalbard: providing baseline data for ecosystems in change. *Polar Biology* **41**, 1995-2005, doi:10.1007/s00300-018-2340-3 (2018).

89 Włodarska-Kowalczuk, M., Pawłowska, J. & Zajączkowski, M. Do foraminifera mirror diversity and distribution patterns of macrobenthic fauna in an Arctic glacial fjord? *Marine Micropaleontology* **103**, 30-39, doi:https://doi.org/10.1016/j.marmicro.2013.07.002 (2013).

90 Gooday, A. J. *et al.* Monothalamous foraminiferans and gromiids (Protista) from western Svalbard: A preliminary survey Published in collaboration with the University of Bergen and the Institute of Marine Research, Norway, and the Marine Biological Laboratory, University of Copenhagen, Denmark. *Marine Biology Research* **1**, 290-312, doi:10.1080/17451000510019150 (2005).

91 Pawłowska, J. *et al.* Palaeoceanographic changes in Hornsund Fjord (Spitsbergen, Svalbard) over the last millennium: new insights from ancient DNA. *Clim. Past* **12**, 1459-1472, doi:10.5194/cp-12-1459-2016 (2016).

92 Kaminski, M. *et al.* Modern agglutinated Foraminifera from the Hovgård Ridge, Fram Strait, west of Spitsbergen: evidence for a deep bottom current. *Annales Societatis Geologorum Poloniae* **85**, 309-320, doi:10.14241/asgp.2015.006 (2015).

93 Langer, M. R., Weinmann, A. E., Lotters, S., Bernhard, J. M. & Rodder, D. Climate-Driven Range Extension of Amphistegina (Protista, Foraminiferida): Models of Current and Predicted Future Ranges. *Plos One* **8** (2013).

94 Dong, S. S., Lei, Y. L., Li, T. G. & Jian, Z. M. Responses of benthic foraminifera to changes of temperature and salinity: Results from a laboratory culture experiment. *Sci China Earth Sci* **62**, 459-472 (2019).

95 Weinmann, A. E. & Goldstein, S. T. Changing structure of benthic foraminiferal communities: implications from experimentally grown assemblages from coastal Georgia and Florida, USA. *Mar Ecol-Evol Persp* **37**, 891-906 (2016).

96 Meslard, F., Bourrin, F., Many, G. & Kerhervé, P. Suspended particle dynamics and fluxes in an Arctic fjord (Kongsfjorden, Svalbard). *Estuarine, Coastal and Shelf Science* **204**, 212-224, doi:https://doi.org/10.1016/j.ecss.2018.02.020 (2018).

97 Csapó, H. K., Grabowski, M. & Węsławski, J. M. Coming home - Boreal ecosystem claims Atlantic sector of the Arctic. *Science of The Total Environment* **771**, 144817, doi:https://doi.org/10.1016/j.scitotenv.2020.144817 (2021).

98 Renaud, P. E. *et al.* Arctic Sensitivity? Suitable Habitat for Benthic Taxa Is Surprisingly Robust to Climate Change. *Frontiers in Marine Science* **6**, doi:10.3389/fmars.2019.00538 (2019).

99 Kujawa, A., Łącka, M., Szymańska, N., Telesiński, M. & Zajączkowski, M. Could Norwegian fjords serve as an analogue for the future of the Svalbard fjords? State and fate of high latitude fjords in the face of progressive "atlantification". *Polar Biology*, doi:10.1007/s00300-021-02951-z (2021).

100 Gooday, A. J., Anikeeva, O. V. & Pawlowski, J. New genera and species of monothalamous Foraminifera from Balaclava and Kazach'ya Bays (Crimean Peninsula, Black Sea). *Marine Biodiversity* **41**, 481-494, doi:10.1007/s12526-010-0075-7 (2011).

101 Altin-Ballero, D. Z., Habura, A. & Goldstein, S. T. *Psammophaga sapela* n. sp., a new monothalamous foraminiferan from coastal Georgia, U.S.A.: Fine structure, gametogenesis, and phylogenetic placement. *Journal of Foraminiferal Research* **43**, 113-126, doi:10.2113/gsjfr.43.2.113 (2013).

102 Smith, C. W. & Goldstein, S. T. The Effects of Selected Heavy Metal Elements (arsenic, Cadmium, Nickel, Zinc) On Experimentally Grown Foraminiferal Assemblages from Sapelo Island, Georgia and Little Duck Key, Florida, U.S.A. *Journal of Foraminiferal Research* **49**, 303-317, doi:10.2113/gsjfr.49.3.303 (2019).

103 Dorst, S. & Schönfeld, J. Diversity Of Benthic Foraminifera on The Shelf and Slope of The NE Atlantic: Analysis of Datasets. *Journal of Foraminiferal Research* **43**, 238-254, doi:10.2113/gsjfr.43.3.238 (2013).

104 Majewski, W., Szczuciński, W. & Zajączkowski, M. Interactions of Arctic and Atlantic water-masses and associated environmental changes during the last millennium, Hornsund (SW Svalbard). *Boreas* **38**, 529-544, doi:https://doi.org/10.1111/j.1502-3885.2009.00091.x (2009).

Supplementary Files

This is a list of supplementary files associated with this preprint. Click to download.

- Nguyenetalsupplementaryinformation21102021.docx
- NguyenetalsupplementarytableS5S821102021.xlsx